MARCH 2016 VOL 12 NO 3
www.nature.com/naturephysics

nature physics

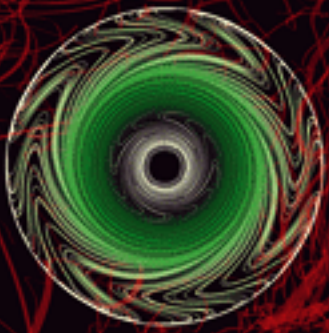

SOLAR PHYSICS
Flux rope knitting

BRANCHED FLOW
Secrets from the ocean floor

QUANTUM MAGNETISM
Avoiding the continuum

Turbulence captured

Big whorls, little whorls

An excursion into ecology and two sets of experiments lay the foundation for our Focus on Turbulence.

The connection between turbulence and predation was made as early as 1922, when Lewis Fry Richardson wrangled it into rhyming verse[1] with the lines:

Big whorls have little whorls
Which feed on their velocity,
And little whorls have lesser whorls
And so on to viscosity.

The poem, later granted wider circulation by James Gleick[2], was a play on Augustus de Morgan's famous paraphrasing[3] of Jonathan Swift:

Great fleas have little fleas
Upon their backs to bite 'em,
And little fleas have lesser fleas
And so ad infinitum.

But the significance of the link lay dormant for some time, surfacing only late last year when Hong-Yan Shih and colleagues came up with a predator–prey model for turbulence, giving the analogy new meaning — and providing evidence in support of some long-held claims about Richardson's whorls.

The paper, which appears on page 245 as part of this month's Focus on Turbulence (see also the News & Views on page 204), reports numerical results that establish a clear link between the transition to turbulence and the universality class describing directed percolation. This idea dates back some thirty years to a conjecture made by Yves Pomeau that the transition to turbulence in shear flows might be understood in terms of an absorbing phase transition. Pomeau provides some historical perspective on this front with a Commentary on page 198.

On the heels of the contribution from Shih *et al.* came a pair of remarkable experimental findings from Masaki Sano and Keiichi Tamai (page 249) and, independently, from Grégoire Lemoult and co-workers (page 254). Although a number of theoretical and experimental studies have lent support to Pomeau's conjecture over the years, no published experimental work had yet confirmed the directed percolation picture. These groups have succeeded in doing so simultaneously, albeit in two vastly different experiments.

Both teams looked at the onset of the transition to turbulence in the shear flow of Newtonian incompressible fluids and found evidence for critical exponents consistent with directed percolation. But whereas Lemoult *et al.* studied flows driven by differential wall motion in a quasi-1D Couette flow geometry, both numerically and experimentally, Sano and Tamai took on 2D channel flow created by a pressure gradient.

Establishing that the transition to turbulence falls into a well-known universality class promises great things for our understanding of this puzzling behaviour. The parallels with other fields are perhaps just as exciting, as our Focus on Turbulence seeks to convey. ❐

References

1. Richardson, L. F. *Weather Prediction by Numerical Process* (Cambridge Univ. Press, 1922).
2. Gleick, J. *Chaos: Making a New Science* (Viking Press, 1987).
3. de Morgan, A. *A Budget of Paradoxes* (Longmans, Green, and Co., 1872).

Grave new world

Physicists have finally detected gravitational waves, in a triumph of ingenuity and perseverance. And now we need to explain them to the general public.

On 14 September 2015, the upgraded Laser Interferometer Gravitational-Wave Observatory (advanced LIGO) made history: the two sites — one in Livingston, Louisiana and the other in Hanford, Washington — detected gravitational waves for the first time since they were predicted 100 years ago by Albert Einstein. The disturbance came from the merger of two black holes of roughly 36 and 29 solar masses, some 1.3 billion light-years away, spiralling inwards, creating a single black hole of 62 solar masses. Keen mathematicians will note that 3 solar masses are missing. That was the energy going into the gravitational waves (equivalent to the total energy from the light of all the stars in the Universe, for 0.02 seconds). As the signal was a brief 'chirp' in the audible frequency range, we can now hear the Universe, whereas previously we could only see it.

Of course, the announcement, made on 11 February 2016, immediately hit the headlines. "We did it", stated David H. Reitze, executive director of LIGO. The excitement was palpable. Some of us cried. But the public's response was largely summed up by the satirical news source, *The Daily Mash,* with their headline: "Scientists completely fail to explain 'gravitational waves'".

And it isn't difficult to explain. Every mass has a gravitational field, and whenever that mass accelerates, the gravitational field changes accordingly. Isaac Newton believed that the fields changed instantaneously on a global scale, but Einstein put a speed limit on the Universe. As information can only travel at the speed of light, information must propagate as a wave — a gravitational wave. These waves convey information on the motion of masses and are complementary to electromagnetic waves that convey information on the motion of charges.

Unfortunately, gravitational waves are weak. Advanced LIGO was able to measure a strain on the order of 10^{-21}. This was only possible due to its recent US$200 million upgrade (involving additional input from the UK, Germany and Australia). But this first detection already tells us so much. Not only do we have a confirmation that black holes of masses greater than 25 solar masses exist, they can do so in a binary system and merge within the lifetime of the Universe. And let's not forget that it is a major, if unsurprising, confirmation of Einstein's general relativity. But what is truly mind-blowing is that not one of the telescopes operating at electromagnetic wavelengths has detected a counterpart event. A black hole merger emits no light, so only a gravitational wave detector was able to sense it.

And with the Virgo interferometer (in Cascina, Italy) coming online, and several other gravitational observatories at other wavelengths in the works, not to mention the Evolved Laser Interferometer Space Antenna (eLISA) (see *Nature Phys.* **11,** 613–615; 2015), we may be able to 'hear' what happened just after the Big Bang, when the Universe was transparent to gravitational waves but not to electromagnetic ones. In the meantime, we should learn to explain the physics of these spectacular events to non-physicists. ❐

nature physics

LETTERS

PUBLISHED ONLINE: 16 NOVEMBER 2015 | DOI: 10.1038/NPHYS3548

Ecological collapse and the emergence of travelling waves at the onset of shear turbulence

Hong-Yan Shih, Tsung-Lin Hsieh and Nigel Goldenfeld*

The mechanisms and universality class underlying the remarkable phenomena at the transition to turbulence remain a puzzle 130 years after their discovery[1]. Near the onset to turbulence in pipes[1], plane Poiseuille flow[2] and Taylor–Couette flow[3], transient turbulent regions decay either directly[4] or through splitting[5–8], with characteristic timescales that exhibit a super-exponential dependence on Reynolds number[9,10]. The statistical behaviour is thought to be related to directed percolation (DP; refs 6,11–13). Attempts to understand transitional turbulence dynamically invoke periodic orbits and streamwise vortices[14–19], the dynamics of long-lived chaotic transients[20], and model equations based on analogies to excitable media[21]. Here we report direct numerical simulations of transitional pipe flow, showing that a zonal flow emerges at large scales, activated by anisotropic turbulent fluctuations; in turn, the zonal flow suppresses the small-scale turbulence leading to stochastic predator–prey dynamics. We show that this ecological model of transitional turbulence, which is asymptotically equivalent to DP at the transition[22], reproduces the lifetime statistics and phenomenology of pipe flow experiments. Our work demonstrates that a fluid on the edge of turbulence exhibits the same transitional scaling behaviour as a predator–prey ecosystem on the edge of extinction, and establishes a precise connection with the DP universality class.

Turbulent fluids are ubiquitous in nature, arising for sufficiently large characteristic speeds U, depending on the kinematic viscosity ν and a characteristic system scale, such as the diameter of a pipe D. Turbulent flows are complex, stochastic, and unpredictable in detail, but transition at lower velocities to a laminar flow, which is simple, deterministic and predictable. This transition is controlled by the dimensionless parameter known as the Reynolds number, which in the pipe geometry of interest here is given by $\mathrm{Re} \equiv UD/\nu$, and occurs in the range $1{,}700 \lesssim \mathrm{Re} \lesssim 2{,}300$. The laminar-turbulence transition has presented a challenge to experiment and theory since Osborne Reynolds' original observation of intermittent 'flashes' of turbulence[1].

To explore this transitional regime, we have performed direct numerical simulations of the Navier–Stokes equations in a pipe of length $L = 10D$, using the open-source code 'Open Pipe Flow'[23], as described in Supplementary Methods. The Reynolds number at which transitional turbulence occurs is higher for short pipes[23], and the simulations reported here for $L = 10D$ were performed at a nominal value $\mathrm{Re} = 2{,}600$, which we estimate to be equivalent to $\mathrm{Re} \lesssim 2{,}200$ in long pipe data[7] based on estimates of when puff decay transitions to puff splitting. We confirmed that our results did not qualitatively change for a longer pipe with $L = 20D$. We denote the time-dependent velocity deviation from the Hagen–Poiseuille flow by $\mathbf{u} = (u_z, u_\theta, u_r)$. Because we were interested in transitional behaviour, we looked for a decomposition[2,6,24,25] of large-scale modes that would indicate some form of collective behaviour, as well as small-scale modes that would be representative of turbulent dynamics. In particular, we report here the behaviour of the velocity field $(\overline{u}_z, \overline{u}_\theta, \overline{u}_r)$, where the bar denotes average over z and θ, and $\overline{u}_r = 0$. We refer to this as the zonal flow. In Fourier space, the zonal flow is given by $\tilde{\mathbf{u}}(k=0, m=0, r)$, where k is the axial wavenumber and m is the azimuthal wavenumber, r is the real space radial coordinate and the tilde denotes Fourier transform in the θ and z directions only. Turbulence was represented by short-wavelength modes, whose energy is $E_\mathrm{T}(t) \equiv (1/2) \sum_{|k|\geq 1, |m|\geq 1} \int |\tilde{\mathbf{u}}(k,m,r)|^2 \, \mathrm{d}V$.

Shown in Fig. 1a is a time series for the energy $E_\mathrm{ZF}(t) \equiv (1/2) \int |\tilde{\mathbf{u}}(0,0,r)|^2 \, \mathrm{d}V$ of the zonal flow, compared with the energy $E_\mathrm{T}(t)$ of the turbulent energy. The curves show clear persistent oscillatory behaviour, modulated by long-wavelength stochasticity, as shown in the phase portrait of Fig. 1b. In Fig. 1c, we have calculated the phase shift between the turbulence and zonal flows, with the result that the turbulent energy leads the zonal flow energy by $\sim \pi/2$. This suggests that these oscillations can be interpreted as a time-series resulting from activator–inhibitor dynamics, such as occurs in a predator–prey ecosystem. Predator–prey ecosystems are characterized by the following behaviour: the 'prey' mode activates the 'predator' mode, which then grows in abundance. At the same time, the growing predator mode begins to inhibit the prey mode. The inhibition of the prey mode starves the predator mode, and it too becomes inhibited. The inhibition of the predator mode allows the prey mode to re-activate, and the population cycle begins again.

The flow configuration for the predator mode is shown in Fig. 1d, and consists of a series of azimuthally symmetric modes with direction reversals as a function of radius r. Such banded shear flows are known as zonal flows and are of special significance in plasma physics, astrophysical and geophysical flows, owing to their role in regulating turbulence[26]. The purely azimuthal component of the zonal flow, denoted by $\overline{u}_\theta(r)$, is spatially uniform in z, and the lack of a radial component means that it is not driven by pressure gradients. Thus, it can exist only as a result of nonlinear interactions with turbulent modes. In this sense, it is a collective mode, one with special significance for transitional turbulence.

The simplest way for such an azimuthal shear flow to couple to turbulent fluctuations is through the Reynolds stress τ: however, a uniform Reynolds stress cannot drive a shear flow, so the first symmetry-allowed possibility is the radial gradient of the Reynolds stress[26], as expressed in the Reynolds momentum equation. Thus, to probe the dynamics that govern the emergence of the zonal flow, we have calculated the time-averaged radial gradient of the instantaneous Reynolds stress, $\tau \equiv u'_\theta u'_r$, where $\mathbf{u}'(z,\theta,r) \equiv \mathbf{u} - \overline{\mathbf{u}}$, and show in Fig. 1f the 4.5-time-unit-running-mean time series of $-\partial_t \overline{u}_\theta$ and the radial gradient $\partial_r \tau$. Both quantities have been averaged over $0 \leq z \leq L$, $0 \leq \theta \leq 2\pi$ and $R_0 \leq r < R$, where $R = D/2$, $R_0 = 0.641R$, and the resulting time series are clearly

Loomis Laboratory of Physics, University of Illinois at Urbana-Champaign, 1110 W. Green Street, Urbana, Illinois 61801, USA. *e-mail: nigel@uiuc.edu

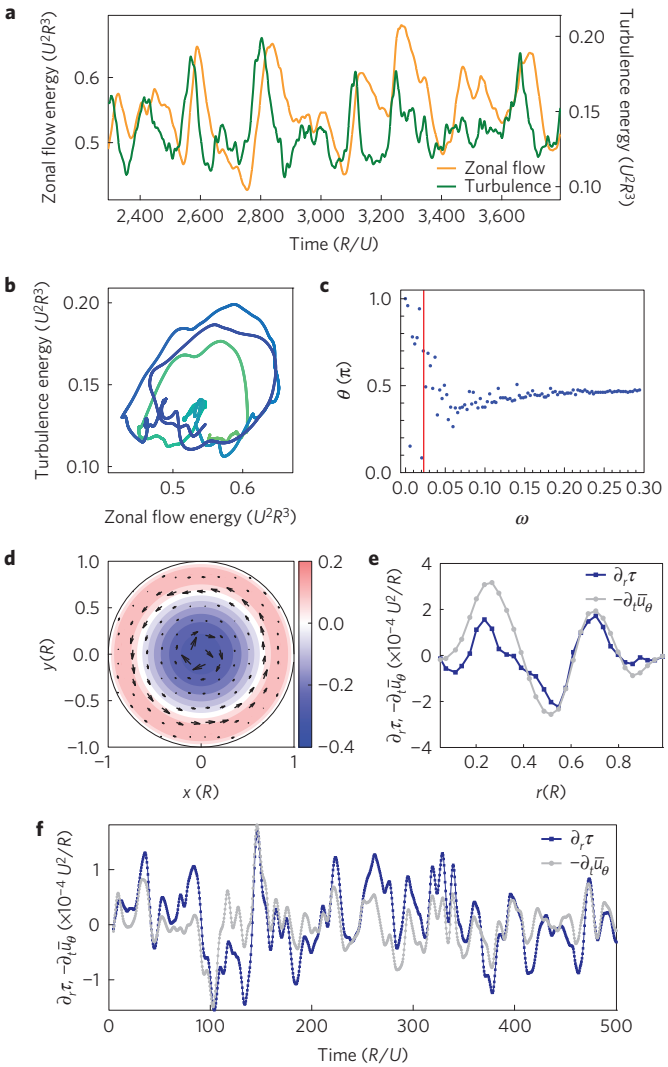

Figure 1 | Predator–prey oscillations in transitional turbulent pipe flow at nominal Re = 2,600, for a pipe of radius $R = D/2$. a, Energy versus time for the zonal flow (orange) and turbulent modes (green). **b**, Phase portrait of the zonal flow and turbulent modes as a function of time, with colour indicating the earliest time in dark blue progressing to the latest time in light green. **c**, Phase shift between the turbulent and zonal flow modes as a function of frequency, showing that the turbulence leads the zonal flow by $\pi/2$, consistent with predator–prey dynamics. The phase shift $\theta(\omega) = \tan^{-1}(\mathrm{Im}[\tilde{C}(\omega)]/\mathrm{Re}[\tilde{C}(\omega)])$ and is shifted to be positive, where $\tilde{C}(\omega)$ is the Fourier transform of the correlation function between the turbulence and the zonal flow in **a**. The red line corresponds to the dominant frequency in the power spectrum. The phase shift near small ω is scatter due to the finite time duration of the time series. **d**, Velocity field configuration of the zonal flow mode $\bar{\mathbf{u}}$. The colour bar indicates the value of $\bar{u}_z$. **e**, Snapshot of the Reynolds stress gradient and zonal flow time derivative as functions of r. **f**, Reynolds stress gradient and zonal flow time derivative as functions of time. The agreement shows that zonal flow dynamics is driven by the radial gradient of the Reynolds stress.

highly correlated. In general, it is the case that zonal flows are driven by statistical anisotropy in turbulence, but are themselves an isotropizing influence on the turbulence through their coupling to the Reynolds stress[27–29]. The fact that turbulence anisotropy activates the zonal flow, and that zonal flow inhibits the turbulence, is responsible for the predator–prey oscillations observed in the numerical simulations.

These numerical results suggest that the large-scale zonal flow and the small-scale turbulence are necessary, and perhaps even sufficient components of an effective coarse-grained description of transitional turbulence in the spirit of Landau theory. Following the usual logic of the modern theory of phase transitions[30], we construct the effective theory from symmetry principles alone, as there are no small parameters with which to perform a systematic derivation. If correct, this effective predator–prey theory should undergo spatio-temporal fluctuations whose functional form matches the observations for the lifetime and splitting time of turbulent puffs in a pipe.

The simplest system that corresponds to our direct numerical simulations of the Navier–Stokes equations has three trophic levels: nutrient (E), Prey (B) and Predator (A), which correspond in the fluid system to laminar flow, turbulence and zonal flow respectively. The interactions between individual representatives of these levels are given by the following reactions:

$$A_i \xrightarrow{d_A} E_i, \quad B_i \xrightarrow{d_B} E_i, \quad A_i + B_j \xrightarrow[\langle ij\rangle]{p} A_i + A_j, \quad B_i + E_j \xrightarrow[\langle ij\rangle]{b} B_i + B_j,$$
$$B_i \xrightarrow{m} A_i, \quad A_i + E_j \xrightarrow[\langle ij\rangle]{D_A} E_i + A_j, \quad B_i + E_j \xrightarrow[\langle ij\rangle]{D_B} E_i + B_j \qquad (1)$$

where d_A and d_B are the death rates of A and B, p is the predation rate, b is the prey birth rate due to consumption of nutrient, $\langle ij\rangle$ denotes hopping to nearest neighbour sites, and D_A and D_B are the nearest-neighbour hopping rate for predator and prey respectively, assumed for simplicity here to be the same value D_{AB} for predator and prey. The 'mutation' term ($B \to A$) is symmetry-allowed and has the interesting consequence that the diagram of the predator–prey model matches that of pipe transitional turbulence (Supplementary Methods).

We simulated this predator–prey model, using methods described in Supplementary Methods, in a thin two-dimensional strip on a 401×11 lattice. The control parameter is the prey birth rate b. When b is small enough, the population is metastable, and cannot sustain itself, decaying with a finite lifetime $\tau^d(b)$. As b increases, the lifetime of the population increases rapidly: in particular the prey lifetime increases rapidly with b. At large enough values of b, the decay of the initial population is not observed, but instead the initially localized population splits after a time $\tau^s(b)$, spreading outwards and spontaneously splitting into multiple clusters, as shown in the space–time plot of clusters of prey of Fig. 2a.

To quantify these observations, we have measured both the lifetime of population clusters in the metastable region and their splitting time using a procedure directly following that of the turbulence experiments and simulations[7], and described in Supplementary Methods. We comment that both timescales involve implicitly measurements of quantities that exceed a given threshold, and thus it is natural that the results are found to conform to extreme value statistics[12,31].

In Fig. 2a we show the phenomenology of the dynamics of initial clusters of prey, corresponding to the predator–prey analogue for the experiments in pipe flow which followed the dynamics of an initial puff of turbulence injected into the flow[4]. Depending on the prey birth rate, the cluster decays either homogeneously or by splitting, precisely mimicking the behaviour of turbulent puffs as a function of Reynolds number. The extraction from data of decay times is described in Supplementary Methods. In Fig. 2b is shown the semi-log plot of lifetime for both decay and splitting as a function of prey birth rate, the upward curvature indicative of super-exponential behaviour. The inset to Fig. 2b shows a double exponential plot of puff lifetime and splitting time versus prey birth rate, the straight line being the fit to the functional form indicated in the caption. These figures indicate a remarkable similarity to the corresponding plots obtained for transitional pipe turbulence in both experiments[4] and direct numerical simulations[7], and demonstrate conclusively that experimental observations are well captured by an effective

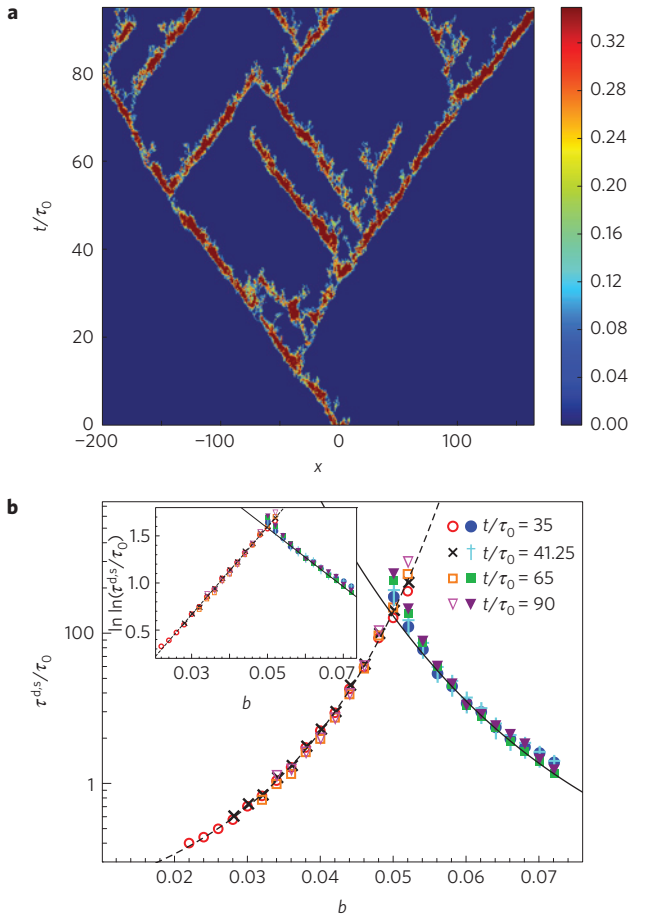

Figure 2 | Stochastic predator–prey model reproduces the phenomenology of transitional pipe turbulence. Lifetime and splitting time of clusters of prey are memoryless processes and obey super-exponential statistics as a function of prey birth rate. To compare with the experiments[4], predator–prey dynamics are performed in a two-dimensional pipe geometry as described in the text. **a**, World line of clusters of prey splitting to form predator–prey travelling waves. The colour measures the local density of prey, corresponding to the intensity of turbulence in pipe flow. In the simulation, the dimensionless parameters are $D_{AB}=0.1, b=0.1, p=0.2, d_A=0.01, d_B=0.01$ and $m=0.001$. In the model simulated, diffusion is isotropic, not biased as would be the case corresponding to a mean flow, where the clusters will accumulate at large times with a well-defined separation set by the depletion zone of nutrient behind each predator–prey travelling wave. **b**, Log lifetime of prey cluster and splitting time as a function of prey birth rate. The upward curvature signifies super-exponential behaviour. The parameters are $D_{AB}=0.01, p=0.1, d_A=0.015, d_B=0.025$ and $m=0.001$. Inset: Double log lifetime versus prey birth rate, showing the fit to the following functional forms: the dashed curve is given by $\tau^d/\tau_0=\exp(\exp(46.539b-0.731))$, and the solid curve is given by $\tau^s/\tau_0=\exp(\exp(-31.148b-3.141))$.

two-fluid model of pipe flow turbulence with predator–prey interactions between the zonal flow and the small scale turbulence.

Our simulations show that the predator–prey model expressed by equation (1) exhibits a rich phase diagram that captures the main features observed in transitional turbulence in pipes. We can understand the qualitative features of the phase diagram from linear stability analysis of the mean field solution of the predator–prey equations[22]. Near the transition, the solutions are linearly stable, all eigenvalues are real and there are no spatial-temporal oscillations. But for higher values of b, the eigenvalues develop an imaginary part, a necessary condition for the breakdown of spatially homogeneous

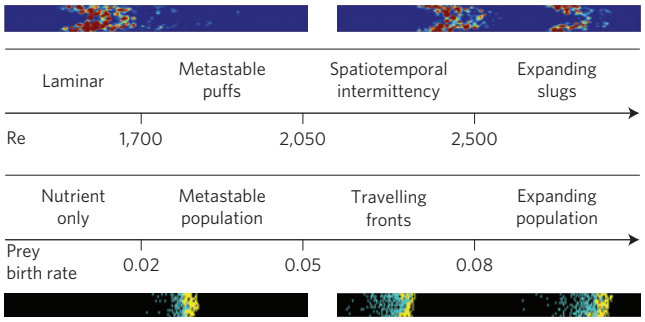

Figure 3 | Schematic phase diagram for transitional pipe turbulence as a function of Reynolds number compared with the phase diagram for predator–prey dynamics as a function of prey birth rate. For each phase is shown a typical flow or predator–prey configuration, indicating the similarity between the turbulent pipe and ecosystem dynamics.

prey domains into periodic travelling wave states[32]. The phase diagram is sketched in Fig. 3, along with the corresponding phase diagram for transitional pipe turbulence as determined by experiment. The phenomenology of the predator–prey system mirrors that of turbulent pipe flow.

To determine the universality class of the non-equilibrium phase transition from laminar to turbulent flow, we use the two-fluid predator–prey mode in equation (1). Near the transition to prey extinction, the prey population is very small and no predator can survive, and thus equation (1) simplifies to

$$B_i \xrightarrow{d_B} E_i, \quad B_i + E_j \xrightarrow[\langle ij\rangle]{b} B_i + B_j, \quad B_i + E_j \xrightarrow[\langle ij\rangle]{D_{AB}} E_i + B_j \qquad (2)$$

These equations are exactly those of the reaction-diffusion model for directed percolation[33]. The argument here is heuristic but the result is correct and can be obtained systematically from statistical field theory techniques, as described in Supplementary Methods.

The observation of the emergence of a zonal flow, excited by the developing turbulent degrees of freedom and the demonstration of its role in determining the phenomenology of transitional pipe turbulence has an interesting consequence: the zonal flow can be assisted by rotating the pipe, and this should catalyse the transition to turbulence, causing it to occur at lower Re. Indeed experiments on axially-rotating pipes[34] are consistent with this prediction.

Our work underscores not only the potential importance of zonal flows in other transitional turbulence situations[9,10], but also shows the utility of coarse-grained effective models for non-equilibrium phase transitions, even to states as perplexing as fluid turbulence.

Received 15 May 2015; accepted 7 October 2015;
published online 16 November 2015

References

1. Reynolds, O. An experimental investigation of the circumstances which determine whether the motion of water shall be direct or sinuous, and of the law of resistance in parallel channels. *Phil. Trans. R. Soc. Lond. A* **174,** 935–982 (1883).
2. Lemoult, G., Gumowski, K., Aider, J.-L. & Wesfreid, J. E. Turbulent spots in channel flow: An experimental study. *Eur. Phys. J. E* **37,** 1–11 (2014).
3. Borrero-Echeverry, D., Schatz, M. F. & Tagg, R. Transient turbulence in Taylor–Couette flow. *Phys. Rev. E* **81,** 025301 (2010).
4. Hof, B., de Lozar, A., Kuik, D. J. & Westerweel, J. Repeller or attractor? Selecting the dynamical model for the onset of turbulence in pipe flow. *Phys. Rev. Lett.* **101,** 214501 (2008).
5. Wygnanski, I., Sokolov, M. & Friedman, D. On transition in a pipe. Part 2: The equilibrium puff. *J. Fluid Mech.* **59,** 283–304 (1975).
6. Moxey, D. & Barkley, D. Distinct large-scale turbulent-laminar states in transitional pipe flow. *Proc. Natl Acad. Sci. USA* **107,** 8091–8096 (2010).
7. Avila, K. *et al.* The onset of turbulence in pipe flow. *Science* **333,** 192–196 (2011).

8. Nishi, M., Bülent, Ü., Durst, F. & Biswas, G. Laminar-to-turbulent transition of pipe flows through puffs and slugs. *J. Fluid Mech.* **614,** 425–446 (2008).
9. Song, B. & Hof, B. Deterministic and stochastic aspects of the transition to turbulence. *J. Stat. Mech.* **2014,** P02001 (2014).
10. Manneville, P. On the transition to turbulence of wall-bounded flows in general, and plane couette flow in particular. *Eur. J. Mech.-B* **49,** 345–362 (2015).
11. Pomeau, Y. Front motion, metastability and subcritical bifurcations in hydrodynamics. *Physica D* **23,** 3–11 (1986).
12. Sipos, M. & Goldenfeld, N. Directed percolation describes lifetime and growth of turbulent puffs and slugs. *Phys. Rev. E* **84,** 035304 (2011).
13. Shi, L., Avila, M. & Hof, B. The universality class of the transition to turbulence. Preprint at http://arXiv.org/abs/1504.03304 (2015).
14. Willis, A. P., Cvitanović, P. & Avila, M. Revealing the state space of turbulent pipe flow by symmetry reduction. *J. Fluid Mech.* **721,** 514–540 (2013).
15. Cvitanović, P. Recurrent flows: The clockwork behind turbulence. *J. Fluid Mech.* **726,** 1–4 (2013).
16. Avila, M., Mellibovsky, F., Roland, N. & Hof, B. Streamwise-localized solutions at the onset of turbulence in pipe flow. *Phys. Rev. Lett.* **110,** 224502 (2013).
17. Kerswell, R. Recent progress in understanding the transition to turbulence in a pipe. *Nonlinearity* **18,** R17–R44 (2005).
18. Eckhardt, B., Schneider, T. M., Hof, B. & Westerweel, J. Turbulence transition in pipe flow. *Annu. Rev. Fluid Mech.* **39,** 447–468 (2007).
19. Chantry, M., Willis, A. P. & Kerswell, R. R. Genesis of streamwise-localized solutions from globally periodic traveling waves in pipe flow. *Phys. Rev. Lett.* **112,** 164501 (2014).
20. Crutchfield, J. P. & Kaneko, K. Are attractors relevant to turbulence? *Phys. Rev. Lett.* **60,** 2715–2718 (1988).
21. Barkley, D. Simplifying the complexity of pipe flow. *Phys. Rev. E* **84,** 016309 (2011).
22. Mobilia, M., Georgiev, I. T. & Täuber, U. C. Phase transitions and spatio-temporal fluctuations in stochastic lattice Lotka–Volterra models. *J. Stat. Phys.* **128,** 447–483 (2007).
23. Willis, A. P. & Kerswell, R. R. Turbulent dynamics of pipe flow captured in a reduced model: Puff relaminarisation and localised 'edge' states. *J. Fluid Mech.* **619,** 213–233 (2009).
24. Prigent, A., Grégoire, G., Chaté, H., Dauchot, O. & van Saarloos, W. Large-scale finite-wavelength modulation within turbulent shear flows. *Phys. Rev. Lett.* **89,** 014501 (2002).
25. Duguet, Y. & Schlatter, P. Oblique laminar-turbulent interfaces in plane shear flows. *Phys. Rev. Lett.* **110,** 034502 (2013).
26. Diamond, P. H., Liang, Y.-M., Carreras, B. A. & Terry, P. W. Self–regulating shear flow turbulence: A paradigm for the *L* to *H* transition. *Phys. Rev. Lett.* **72,** 2565–2568 (1994).
27. Sivashinsky, G. & Yakhot, V. Negative viscosity effect in large-scale flows. *Phys. Fluids* **28,** 1040–1042 (1985).
28. Bardóczi, L., Bencze, A., Berta, M. & Schmitz, L. Experimental confirmation of self-regulating turbulence paradigm in two-dimensional spectral condensation. *Phys. Rev. E* **90,** 063103 (2014).
29. Parker, J. B. & Krommes, J. A. Generation of zonal flows through symmetry breaking of statistical homogeneity. *New J. Phys.* **16,** 035006 (2014).
30. Goldenfeld, N. *Lectures On Phase Transitions and the Renormalization Group* (Addison-Wesley, 1992).
31. Goldenfeld, N., Guttenberg, N. & Gioia, G. Extreme fluctuations and the finite lifetime of the turbulent state. *Phys. Rev. E* **81,** 035304 (2010).
32. Dunbar, S. R. Travelling wave solutions of diffusive Lotka–Volterra equations. *J. Math. Biol.* **17,** 11–32 (1983).
33. Ódor, G. Universality classes in nonequilibrium lattice systems. *Rev. Mod. Phys.* **76,** 663–724 (2004).
34. Murakami, M. & Kikuyama, K. Turbulent flow in axially rotating pipes. *J. Fluids Eng.* **102,** 97–103 (1980).

Acknowledgements

We gratefully acknowledge helpful discussions with Y. Duguet and Z. Goldenfeld. We especially thank A. Willis for permission to use his code 'Open Pipe Flow'[23]. This work was partially supported by the National Science Foundation through grant NSF-DMR-1044901.

Author contributions

H.-Y.S. and N.G. designed the project. Computer simulations of pipe turbulence were performed by T.-L.H. Computer simulations of stochastic predator–prey dynamics were performed by H.-Y.S. All authors contributed to the interpretation of the data and the writing of the paper.

Additional information

Supplementary information is available in the online version of the paper. Reprints and permissions information is available online at www.nature.com/reprints. Correspondence and requests for materials should be addressed to N.G.

Competing financial interests

The authors declare no competing financial interests.

nature physics

SUPPLEMENTARY INFORMATION

DOI: 10.1038/NPHYS3548

Ecological collapse and the emergence of traveling waves at the onset of shear turbulence

Hong-Yan Shih,[1] Tsung-Lin Hsieh,[1] Nigel Goldenfeld[1*]

[1]*Loomis Laboratory of Physics, University of Illinois at Urbana-Champaign, 1110 W. Green St., Urbana, IL 61801, USA*

Supplementary Methods

Direct numerical simulations of the Navier-Stokes equations.

We performed direct numerical simulations (DNS) of the Navier-Stokes equations in a pipe, using the open-source code "Open Pipe Flow"[1]. The equations were solved using a pseudo-spectral method in cylindrical coordinates[1], having 60 grid points in the radial (r) direction, 32 Fourier modes in the azimuthal (θ) direction and 128 modes in the axial (z) direction. Such a model is of course a reduced description of reality, but the main features can be well captured, with a slight renormalization of the Re needed to compare with experiment[1]. For the accuracy required in our study, we used 32 modes in the azimuthal direction[1]. The spatial resolutions were chosen such that the resolvable power spectra span over six orders of magnitude. The pipe length L is 10 times its diameter D, with periodic boundary conditions in the z direction[1]. With this resolution, the transition to turbulence occurs in a range of Re numbers between 2200 and 3000, and moves to smaller Re at still higher resolution. To try and relate the nominal Reynolds number in our finite length pipe simulations to the values reported in experiments or simulations with longer pipes, we found that we could observe puff decay up to about $\mathrm{Re}_{\mathrm{nominal}} \sim 2400$, whereas the experimental

DOI: 10.1038/NPHYS3548

threshold for puff decay is about 2000. Thus, we can estimate that the nominal Reynolds number, $\mathrm{Re}_{\mathrm{nominal}} = \mathrm{Re}_{\mathrm{experiment}} + \Delta\mathrm{Re}$, with $\Delta\mathrm{Re} \sim 400$ for $L = 10D$. We report here measurements at $\mathrm{Re} = 2600$, slightly above the transition[2]. The mass flux and $\mathrm{Re} = 2600$ were held constant in time[1]. The laminar flow is the Hagen–Poiseuille flow, which was independent of time as the mass flux was held constant[1]. Therefore the data we show in Fig. 1 with Re = 2600 for $L = 10D$ are consistent with the puff-splitting regime in the pipe flow experiments, and well below the regime where the pipe is completely filled with turbulence.

Stochastic simulations of predator-prey dynamics.

The specific system has three trophic levels: nutrient (E), Prey (B) and Predator (A), which correspond in the fluid system to laminar flow, turbulence and zonal flow respectively. Such a system can be naively modeled by the Lotka-Volterra ordinary differential equations[3–5], which in the case of ecosystems with finite resources do not permit long-time persistent oscillatory solutions, unless additional biological details such as functional response are included. In fact, it is necessary to include the dynamics of individual birth-death events, and when this is done correctly, it is found that the number fluctuations drive the population oscillations[6] through resonant amplification. Thus, we use a stochastic model at the outset.

The interactions between individual representatives of these levels are given by the following rate equations

$$A_i \xrightarrow{d_{\mathrm{A}}} E_i, \qquad B_i \xrightarrow{d_{\mathrm{B}}} E_i, \qquad A_i + B_j \xrightarrow[\langle ij\rangle]{p} A_i + A_j, \qquad B_i + E_j \xrightarrow[\langle ij\rangle]{b} B_i + B_j,$$
$$B_i \xrightarrow{m} A_i, \qquad A_i + E_j \xrightarrow[\langle ij\rangle]{D_{\mathrm{A}}} E_i + A_j, \quad B_i + E_j \xrightarrow[\langle ij\rangle]{D_{\mathrm{B}}} E_i + B_j. \tag{S1}$$

where d_{A} and d_{B} are the death rates of A and B, p is the predation rate, b is the prey birth rate due to consumption of nutrient, $\langle ij\rangle$ denotes hopping to nearest neighbor sites, D_{A} and D_{B} are the nearest-neighbor hopping rate for predator and prey respectively, assumed for simplicity here

to be the same value D_{AB} for predator and prey. We found that our results are not sensitive to this assumption, presumably because the predator number is small in the transitional regime. In addition to the familiar term that describes how the prey act as a source (activate) for the predators ($AB \to AA$), we have introduced another low order in population number, symmetry-allowed term ($B \to A$) with rate m; both of these terms model the induction of the zonal flow from the turbulence degrees of freedom, but the latter one is conventionally omitted in ecosystem contexts, because it would represent a phenotypic switch such as the mutation of the prey into predator (in rapid evolution contexts such terms can be relevant[7]). We include it here, not only because there is no special reason to exclude it, but because its presence ensures that the phase diagram of the predator-prey ecosystem shows a transition from extinction (laminar) to coexistence of predator (zonal flow) and prey (turbulence). Without this term, the predator-prey equations have an intermediate phase where the prey survive off the nutrient but the predators are dead. We have not observed such a phase (puffs of turbulence without zonal flow) in our DNS, and so conclude that the induction of zonal flow by turbulence does indeed occur through this low order mechanism too. We are primarily interested in long-wavelength properties of the system, at least in the vicinity of the turbulence transition, where we expect the transverse correlation length to be larger than the pipe diameter, implying that the behavior is in fact quasi-one-dimensional. The crossover phenomena associated with this have been discussed previously[8], and thus our two-dimensional strip model should be appropriate and quantitatively correct near the transition.

We simulated these equations on a 401×11 lattice (strip) in two dimensions, intended to emulate the pipe geometry. Lattice sites were only allowed to be occupied by one of E, A or B. The predator (A) and prey (B) are additionally allowed to diffuse via random walk on the lattice with diffusion coefficient $D_{\mathrm{AB}} = 0.1$ in units of the square of the lattice spacing divided by the time step (set equal to unity). The initial conditions for the simulations were a random population of prey and predator, occupying with probability $4/5$ and $1/5$ respectively on the lattice sites between

DOI: 10.1038/NPHYS3548

$x \in [-15, 15]$ and $y \in [-5, 5]$ where x labels the direction along the axis of the ecosystem (pipe) and y labels the transverse direction. The predator-prey dynamics in Eq. S1 was implemented by the following algorithm: at each time step, a site i is randomly chosen, a random number s, is generated from the uniform distribution between zero and one. The behavior on the site is decided by the random number: (1) if $s < 1/6$ and the site i is occupied by any individual, and if a randomly chosen neighbor site is empty, then that individual diffuses to the random neighboring site with rate $\mu = 0.01$ (i.e. this reaction happens if another uniformly distributed random number is less than $1 - \exp \mu$); (2) if $1/6 \leq s < 1/3$ and the site i is occupied by a prey individual, and if a randomly chosen neighbor site, j, is empty, then one prey individual is born on the site j with rate b; (3) if $1/3 \leq s < 1/2$ and the site i is occupied by a predator individual, and if a randomly chosen neighbor site, j, is occupied by a prey individual, then the prey individual is replaced by a new-born predator individual with rate p; (4) if $1/2 \leq s < 2/3$ and the site i is occupied by a predator individual, that predator individual dies with rate d_{A}; (5) if $2/3 \leq s < 5/6$ and the site i is occupied by a prey individual, that prey individual dies with rate d_{B}; (6) if $5/6 \leq s < 1$ and the site i is occupied by a prey individual, then the prey individual is replaced by a predator individual with rate m. Then within the same time step, the above processes are repeated 401×11 times so that on average one reaction takes place at each lattice site in the system.

Measurement of decay and splitting lifetimes.

We measured both the lifetime of population clusters in the metastable region and their splitting time using a procedure directly following that of the turbulence experiments and simulations[2]. To this end, we monitor the coarse-grained prey population density $\tilde{n}_B(i) = \sum_{j=-J}^{j=J} \sum_{l=-H/2}^{l=H/2} n_B(i + j, l)/(H + 1)/(2J + 1) - 0.25$, where H is the height of the system (11 lattice units) and $J = 3$. The lifetime of prey clusters is defined as the time it takes for the last prey individual to die. The cluster splitting time is defined as the first time that the distance between the edges of two coarse-

grained prey clusters exceed 25 unit sites. We comment that both timescales involve implicitly measurements of quantities that exceed a given threshold, and thus it is natural that the results are found to conform to extreme value statistics[8,9].

In Figure S1 we show the phenomenology of the dynamics of initial clusters of prey, corresponding to the predator-prey analogue for the experiments in pipe flow which followed the dynamics of an initial puff of turbulence injected into the flow[10]. Depending upon the prey birth rate, the cluster decays either homogeneously or by splitting, precisely mimicking the behavior of turbulent puffs as a function of Reynolds number. Figure S1 (a) and (b) show that the decay is exponential in time, indicating that it is a memoryless process with a single time constant. Figure S1 (c) and (d) show that the survival probability is a sigmoidal curve, whose inverse lifetime as a function of prey birth rate is plotted in a log-linear scale in Figures S1 (e) and (f). If the lifetime were an exponential function, this curve would be a straight line with negative slope. The downward curvature is a manifestation of super-exponential behavior. These figures indicate a remarkable similarity to the corresponding plots obtained for transitional pipe turbulence in both experiments[10] and direct numerical simulations[2], and demonstrate conclusively that experimental observations are well captured by an effective two-fluid model of pipe flow turbulence with predator-prey interactions between the zonal flow and the small scale turbulence.

Derivation of directed percolation from predator-prey model

In order to determine the universality class of the non-equilibrium phase transition from laminar to turbulent flow, we use the two-fluid predator-prey mode in Equations (S1). Near the transition to prey extinction, the prey population is very small and no predator can survive, and thus Equations (S1) can be simplified to

$$B_i \xrightarrow{d_B} E_i, \qquad B_i + E_j \xrightarrow[\langle ij \rangle]{b} B_i + B_j, \qquad B_i + E_j \xrightarrow[\langle ij \rangle]{D_{AB}} E_i + B_j. \tag{S2}$$

DOI: 10.1038/NPHYS3548

These equations are exactly those of the reaction-diffusion model for directed percolation[11,12]. A more detailed and systematic way to reach this conclusion is to represent Equations (S1) exactly in path integral form using the Doi formalism[12–17]. The resulting action simplifies near the transition to that of Reggeon field theory[18,19], which has been shown to be in the universality class of directed percolation[20,21]. Numerical simulations of 3 + 1 dimensional directed percolation in a pipe geometry have reproduced the statistics and behavior of turbulent puffs and slugs in pipe flow[8,22], and a detailed comparison between theory and numerical simulation in Couette flow has been reported[23]. The super-exponential behavior of DP might seem to contradict the expectation based upon the known critical behavior[24]. However, it is important to recognize that the usual exponents relate to DP starting from a single seed, whereas the experiments and simulations are conducted with an extended seed that has a finite length or number of seed points. These points behave as independent identically-distributed random variables as long as the transverse correlation length is much smaller than the seed size, but once the correlation length is of order the seed size, the seed is effectively a single correlated extended source, and once the correlation length is much larger than this size, there will be a crossover to the usual DP exponents.

References

1. Willis, A. P. & Kerswell, R. R. Turbulent dynamics of pipe flow captured in a reduced model: puff relaminarisation and localised 'edge' states. *J. Fluid Mech.* **619**, 213–233 (2009).

2. Avila, K. *et al.* The onset of turbulence in pipe flow. *Science* **333**, 192–196 (2011).

3. Lotka, A. J. Contribution to the theory of periodic reactions. *The Journal of Physical Chemistry* **14**, 271–274 (1910).

4. Volterra, V. *Variazioni e fluttuazioni del numero d'individui in specie animali conviventi* (C. Ferrari, 1927).

5. Renshaw, E. *Modelling biological populations in space and time*, vol. 11 (Cambridge University Press, 1993).

6. McKane, A. J. & Newman, T. J. Predator-prey cycles from resonant amplification of demographic stochasticity. *Physical Review Letters* **94**, 218102 (2005).

7. Shih, H.-Y. & Goldenfeld, N. Path-integral calculation for the emergence of rapid evolution from demographic stochasticity. *Physical Review E* **90**, 050702 (2014).

8. Sipos, M. & Goldenfeld, N. Directed percolation describes lifetime and growth of turbulent puffs and slugs. *Physical Review E* **84**, 035304 (2011).

9. Goldenfeld, N., Guttenberg, N. & Gioia, G. Extreme fluctuations and the finite lifetime of the turbulent state. *Phys. Rev. E* **81**, 035304 (2010).

10. Hof, B., de Lozar, A., Kuik, D. J. & Westerweel, J. Repeller or attractor? Selecting the dynamical model for the onset of turbulence in pipe flow. *Phys. Rev. Lett.* **101**, 214501 (2008).

11. Hinrichsen, H. Non-equilibrium critical phenomena and phase transitions into absorbing states. *Advances in Physics* **49**, 815–958 (2000).

DOI: 10.1038/NPHYS3548

12. Ódor, G. Universality classes in nonequilibrium lattice systems. *Reviews of Modern Physics* **76**, 663 (2004).

13. Doi, M. Second quantization representation for classical many-particle system. *Journal of Physics A: Mathematical and General* **9**, 1465–1477 (1976).

14. Grassberger, P. & Scheunert, M. Fock-space methods for identical classical objects. *Fortschritte der Physik* **28**, 547–578 (1980).

15. Mikhailov, A. Path integrals in chemical kinetics I. *Physics Letters A* **85**, 214–216 (1981).

16. Goldenfeld, N. Kinetics of a model for nucleation-controlled polymer crystal growth. *Journal of Physics A Mathematical General* **17**, 2807–2821 (1984).

17. Mattis, D. C. & Glasser, M. L. The uses of quantum field theory in diffusion-limited reactions. *Reviews of Modern Physics* **70**, 979–1001 (1998).

18. Mobilia, M., Georgiev, I. T. & Täuber, U. C. Phase transitions and spatio-temporal fluctuations in stochastic lattice Lotka-Volterra models. *Journal of Statistical Physics* **128**, 447–483 (2007).

19. Täuber, U. C. Population oscillations in spatial stochastic Lotka–Volterra models: a field-theoretic perturbational analysis. *Journal of Physics A: Mathematical and Theoretical* **45**, 405002 (2012).

20. Cardy, J. L. & Sugar, R. L. Directed percolation and reggeon field theory. *Journal of Physics A: Mathematical and General* **13**, L423–L427 (1980).

21. Janssen, H. On the nonequilibrium phase transition in reaction-diffusion systems with an absorbing stationary state. *Zeitschrift für Physik B Condensed Matter* **42**, 151–154 (1981).

22. Allhoff, K. T. & Eckhardt, B. Directed percolation model for turbulence transition in shear flows. *Fluid Dynamics Research* **44**, 031201 (2012).

23. Shi, L., Avila, M. & Hof, B. The universality class of the transition to turbulence. *arXiv preprint arXiv:1504.03304* (2015).

24. Hinrichsen, H. H. Non-equilibrium critical phenomena and phase transitions into absorbing states. *Advances in Physics* **49**, 815–958 (2000).

DOI: 10.1038/NPHYS3548

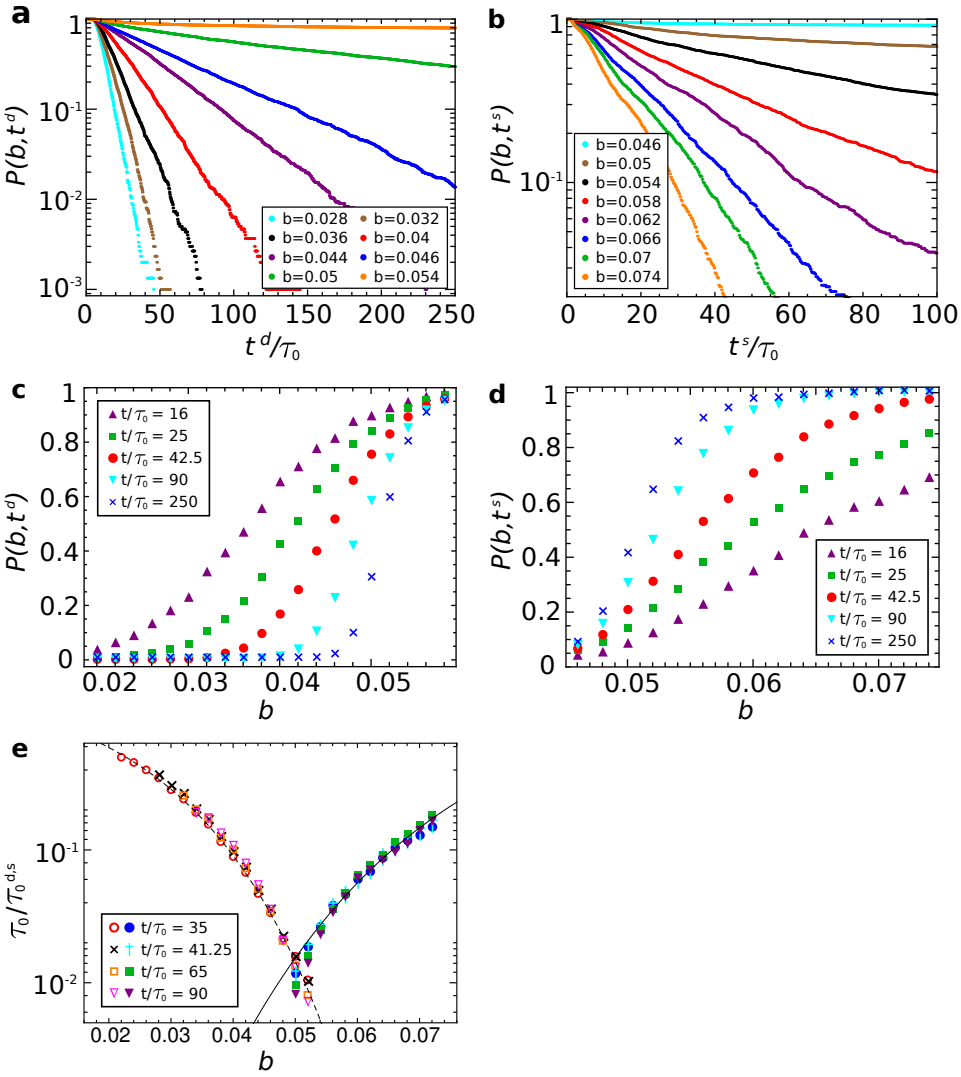

Figure S1: Stochastic predator-prey model reproduces the phenomenology of transitional pipe turbulence. Lifetime and splitting time of clusters of prey are memoryless processes and obey super-exponential statistics as a function of prey birth rate. To compare with the experiments[10], predator-prey dynamics are performed in two-dimensional pipe geometry as described in the text. The dimensionless parameters in the simulation are $D_{\mathrm{AB}} = 0.01, p = 0.1, d_{\mathrm{A}} = 0.015, d_{\mathrm{B}} = 0.025$ and $m = 0.001$. (a) Log survival probability of prey cluster vs. time during homogeneous decay to extinction. Here the characteristic time scale that is estimated by $\tau_0 \sim 200$. (b) Log survival probability of prey cluster vs. time during decay to splitting. (c) Survival probability of prey cluster as a function of prey birth rate during homogeneous decay to extinction. (d) Survival probability of prey cluster as a function of prey birth rate during decay to splitting. (e) Log inverse lifetime of prey cluster, as a function of prey birth rate during homogeneous decay to extinction (left curve, τ^{d}) and during decay to splitting (right curve, τ^{s}). The dashed curve is given by $\tau_0/\tau^{\mathrm{d}} = 1/\exp(\exp(46.539b - 0.731))$, and the solid curve is given by $\tau_0/\tau^{\mathrm{s}} = 1/\exp(\exp(-31.148b - 3.141))$.

Transition to turbulence

As any physicist knows, fluid in a pipe can flow smoothly at sufficiently low speeds, as parcels of fluid trace out continuous streamlines. At higher speeds, the simple flow often becomes turbulent, with fluid elements now moving on disorderly, chaotic paths. In 1883, the British physicist Osborne Reynolds tried to clarify details of this transition, along the way introducing his Reynolds number, Re, as a key dimensionless quantity characterizing flows by the relative importance of inertial and viscous forces.

Today, physicists still lack a theory, based on first principles, explaining the nature of this transition. Even so, remarkable progress has been made in the past decade, and turbulence in pipe flow is finally yielding some of its secrets.

Naively, one might imagine that the stable, laminar flow simply becomes unstable at sufficient flow speeds — or, equivalently, a high enough Reynolds number, Re. Yet, according to the Navier-Stokes equations, the laminar state is in fact always linearly stable. When disturbed vigorously, turbulence in pipes begins at Re ~ 2,000, whereas in especially quiescent conditions, the transition can be delayed to Re ~ 12,000 or even higher.

This confusing situation motivated Reynolds in his 1883 work to define the turbulent transition — linked to the critical Reynolds number, Re_c — as the point beyond which turbulence, once started, will persist indefinitely. Turbulence can exist, or not exist, both below and above the critical threshold. For $Re < Re_c$, it always dies out eventually, while for $Re > Re_c$, turbulence once created persists.

So how does this transition come about? In a series of experiments over the past decade, physicists have pinned down a number of telling empirical details. To begin with, at low Re, turbulence always settles into a simple form — it exists not as a spatially extended pattern, but in localized 'puffs', separated by laminar zones. The typical lifetime of a puff seems to increase with Re in a faster-than-exponential way. Even so, this lifetime — at least within the limits of experiment — always remains finite (B. Hof *et al.*, *Nature* **443,** 59–62; 2006).

One might have imagined persistent turbulence arising from a finite Re divergence of this lifetime, but that is not the case. Rather, something else seems to happen: puffs at higher Re not only last longer, but also begin to split apart, making turbulence spread. The rate at which puffs split apart also increases with Re, again in a faster-than-exponential way (K. Avila *et al.*, *Science* **333,** 192–196; 2011), and it is the combination of these two trends — puffs lasting longer and splitting more quickly — that lies behind the transition to lasting turbulence. Below the critical Re, puffs die out more quickly than they split to generate new ones. Turbulence dies out. Above the critical Re, the splitting happens faster than the dying out, and turbulence persists.

Turbulence in pipe flow is finally yielding some of its secrets.

Intriguingly, there is a close similarity with the dynamics of epidemics. Moving Re up through the critical value is like increasing the basic reproduction number for an infectious agent through the critical point so that each new infection ultimately creates more than one further infection, and the agent becomes endemic.

This picture of turbulence gains further support from theoretical approaches. Thirty years ago, French physicist Yves Pomeau suggested that the coarse-grained features of how turbulent and laminar zones mingle in regimes of mixed flow might act like patterns in so-called directed percolation. This is a fundamental stochastic spreading process linked to phenomena ranging from fluid movement through porous media to forest fires. Inspired by this idea, mathematician Dwight Barkley of the University of Warwick recently proposed a model for pipe flow in which turbulent puffs behave rather like action potentials in nerve axons. The state of linearly stable laminar flow would be the medium rest state, with turbulence the excited state.

A model based on this picture (D. Barkley *Phys. Rev. E* **84,** 016309; 2011) shows a continuous transition to sustained turbulence at a critical value of Re_c. The mean puff lifetime grows with Re, as does the rate of splitting, and just above Re_c, a puff is more likely to split than to decay. Just above the critical point, Barkley found, the fraction of fluid in the turbulent phase grows as $(Re - Re_c)^{0.28}$. This is just as expected if the transition really is in the class of directed percolation, as Pomeau proposed. More recently, Barkley and colleagues have taken this approach further (D. Barkley *et al.* *Nature* **526,** 550–553; 2015), offering a simple dynamical system that accounts for even more features of pipe flow, including how puffs grow wider with time as they flow downstream.

An alternative — and quite different theoretical perspective — points to directed percolation as well. Nigel Goldenfeld and colleagues (*Nature Phys.* http://doi.org/96m; 2015) ran numerical simulations of pipe flow and tried to identify the most important non-turbulent collective modes. These turned out to be so-called 'zonal flows' representing azimuthal modulations of the basic laminar flow pattern. These zonal flows represent important coherent ways that energy often seems to get organized in these pipe flows.

From these observations, the researchers noted that these zonal flows compete with turbulence following a basic predator–prey interaction. In this picture, the basic laminar flow is akin to a nutrient, which turbulence (the prey species) feeds on and spreads. In turn, turbulence can be fed on by the zonal flows (the predator species). Studying the simplest model for such interactions, the authors found that it leads to distributions of puff lifetimes and splitting times that look very much like those found for pipe flow. In this case, the parameter playing the role of Re is the prey (or turbulent puff) birth rate.

Again, as it turns out, this simple predator–prey model maps onto a statistical model in the directed percolation class. So Pomeau's conjecture seems to be on target, and supported from two different points of view. It seems that at least one small part of the long quest to understanding the transition to turbulence may be coming nearer to a close. At the same time, much less remains known about turbulence at very high Re, far away from the transition regime.

These results are also satisfying as directed percolation is thought to be the general universality class for non-equilibrium phase transitions with an absorbing state — a state that, once entered, is never left. Surprisingly, turbulence in pipe flow may be the first good experimental example. ❐

MARK BUCHANAN

FLUID DYNAMICS

In pursuit of turbulence

In the transition from laminar to turbulent pipe flow, puffs of turbulence form, split and decay. The phenomenology and lifetime of these turbulent puffs exhibit population dynamics that also drive predator–prey ecosystems on the edge of extinction.

Johannes Knebel, Markus F. Weber and Erwin Frey

Turbulence can be quite a nuisance, bothering both travellers on a plane and physicists in the kitchen. The flow of water from a tap reminds us that despite our knowledge about the oscillations of neutrinos and cosmic inflation, we know very little about the transition to turbulence that occurs right in front of us. At first, the water flows smoothly, but once the tap is opened more, the flow becomes chaotic. Experiments probing the transition from laminar to turbulent flow began in 1883 with Reynolds[1,2] and continue to this day[3]. Now, writing in *Nature Physics*, Hong-Yan Shih and colleagues have taken an important step towards understanding this transition[4], by borrowing ideas from ecology.

The researchers identified a nonlinear feedback between different energy modes as the main driver of the transition. This feedback is seen as a hunt: turbulent modes are a prey that is hunted by a collective predator mode. When the prey is on the edge of extinction, the predator–prey ecosystem exhibits the same statistical properties as the fluid on the edge of turbulence, providing a link between transitional turbulence and directed percolation.

When a fluid flows through a pipe, its phenomenology changes dramatically with the flow speed. At a low speed (low Reynolds number, Re), the fluid flows smoothly in a laminar fashion, whereas at higher speeds (high Re), the flow becomes turbulent. In the transition from laminar to turbulent flow, localized pockets of chaos, so-called puffs, form spontaneously in the laminar flow. These puffs decay again and fade back into the laminar flow after a mean time τ_d that increases super-exponentially with Re ($\tau_d \propto \exp[\exp(\mathrm{Re})]$). However, puffs can also split spontaneously by nucleating an offspring puff further downstream. The mean splitting time τ_s decreases super-exponentially with Re ($\tau_s \propto \exp[\exp(-\mathrm{Re})]$) (ref. 5). Thus, with increasing Re, splitting becomes much more probable than decaying — and turbulence wins.

The theorist's basic tool to approach the flow of a fluid through a pipe is the Navier–Stokes equation, which describes the competition between viscous dissipation and inertia. Interestingly, the transition from laminar to turbulent flow sets in without a linear instability of the Navier–Stokes equation; small perturbations to the laminar flow decay for all Reynolds numbers. This is in contrast to other phenomena in fluid dynamics, such as the self-organization of Rayleigh–Bénard cells, which arise out of a linear instability of the Navier–Stokes equation. The lack of linear instability makes the transition to turbulence hard to grasp and interpret conceptually.

Shih *et al.*[4] studied pipe flow by numerically solving the Navier–Stokes equation and observed some startling new patterns that differ from the previously observed longitudinal vortices[6] or the changes in mean profile[7]. These patterns form in the transitional regime between laminar and turbulent flow and are the signature of a collective energy mode. This large-scale pattern of the flow, called zonal flow, is activated by anisotropic turbulent fluctuations. Curiously, these fluctuations are in turn inhibited by the zonal flow, resulting in dynamics that resemble an evolutionary predator–prey cycle.

The researchers showed that the analogy to population dynamics is not only a shallow caricature of the true fluid dynamics. In fact, the roles of predator and prey can be ascribed to the above modes of the flow's Fourier spectrum. Shih *et al.*[4] thereby obtained a coarse-grained description of the energy transport in the fluid flow in terms of a predator–prey model. The zonal flow plays the role of the predator hunting the turbulent modes as its prey. In turn, the turbulent modes feed on the laminar flow as their nutrient source. A population of predator and prey goes extinct for a low birth rate of the prey, whereas long-lived oscillations are observed for higher birth rates.

As the researchers demonstrated, both the lifetime and the splitting time of prey clusters follow the same super-exponential statistics as the lifetime and splitting time of turbulent puffs. Thus, the predator–prey ecosystem on the edge of extinction shows the same statistics as a fluid on the edge of turbulence. The birth rate of the prey controls the transition between extinction and survival, as does the Reynolds number for the transition between laminar and turbulent flow. Based on their population model, Shih *et al.*[4] also substantiated a link between transitional turbulence and directed percolation, which had been conjectured almost 30 years ago[8].

It is a common theme in physics that interactions on the microscopic scale yield effective nonlinear feedbacks on the macroscopic scale. Often, population dynamics turns out to be a suitable model to describe such emerging nonlinear behaviour. The self-regulation of shear flow turbulence in plasma physics[9] and the competition between quantum states in driven–dissipative condensation of bosons[10] are just two examples for the successful application of population dynamics.

In this lithograph by Arthur Rackham (*The Rhine's pure gleaming children told me of their sorrow*, 1910), the sleek, floating hair of the three water nymphs, the Rhinemaidens, contrasts the wild, blazing hair of Loge ('fire' in Old Norse), an ally of the gods in Norse mythology. Shih *et al.*[4] explain how the transition from the sleek, laminar flow of a fluid to a wild, turbulent state can be understood with the help of population dynamics. Image inspired by ref. 11.

Capturing the transition from laminar to turbulent flow on a macroscopic level by a predator–prey model now establishes another fascinating example of this theme.

Nevertheless, many puzzles about turbulence and fluid flow in general still remain. Although the Navier–Stokes equation provides a fully accepted mathematical description for fluid dynamics on an enormously broad range of length and time scales, the understanding of physical principles underlying particular phenomena, such as transitional turbulence, requires coarse-grained descriptions. It seems that we need 'reduced' descriptions at some special points in the parameter space of the Navier–Stokes equation to fathom these principles. Why is this so? A physicist trained in the age of renormalization group theory might reply that it is because there are 'critical points' at which universal models are an appropriate way of approaching the problem. But why are there those critical points in the first place, and are there really critical points in fluid turbulence? At present we lack a deeper understanding of mathematical models, such as the Navier–Stokes equation and its cousins for more complex fluids, to answer this question. Further research is certainly needed to unravel the secrets of turbulence and the hidden surprises of tap water. ❐

Johannes Knebel, Markus F. Weber and Erwin Frey are in the Arnold-Sommerfeld-Center for Theoretical Physics and Center for NanoScience at Ludwig-Maximilians-Universität München, Theresienstrasse 37, D-80333 Munich, Germany.
e-mail: frey@lmu.de

References

1. Reynolds, O. *Phil. Trans. R. Soc. Lond.* **174,** 935–982 (1883).
2. Reynolds, O. *Phil. Trans. R. Soc. Lond. A* **186,** 123–164 (1895).
3. Barkley, D. *et al. Nature* **526,** 550–553 (2015).
4. Shih, H.-Y., Hsieh, T.-L. & Goldenfeld, N. *Nature Phys.* **12,** 245–248 (2016).
5. Avila, K. *et al. Science* **333,** 192–196 (2011).
6. Schneider, T. M., Eckhardt, B. & Vollmer, J. *Phys. Rev. E* **75,** 066313 (2007).
7. Barkley, D. *Phys. Rev. E* **84,** 016309 (2011).
8. Pomeau, Y. *Physica D* **23,** 3–11 (1986).
9. Diamond, P. H., Liang, Y.-M., Carreras, B. A. & Terry, P. W. *Phys. Rev. Lett.* **72,** 2565–2568 (1994).
10. Knebel, J., Weber, M. F., Krüger, T. & Frey, E. *Nature Commun.* **6,** 6977 (2015).
11. Ball, P. *Flow* (Oxford Univ. Press, 2009).

QUANTUM FERROFLUIDS

Made to order

Hydrodynamics and magnetism meet spectacularly in ferrofluids — liquids containing magnetic nanoparticles. The ferrohydrodynamic magic happens when an amount of ferrofluid is put on a superhydrophobic surface and exposed to a magnetic field. The forces at play, notably the liquid's surface tension and the tendency of the magnetic particles to align with the field, result in a hedgehog-like droplet crystal (pictured). Holger Kadau and colleagues have now observed this phenomenon, known as the Rosensweig instability, for a quantum ferrofluid (*Nature* http://doi.org/bcf4; 2016) — a Bose–Einstein condensate (BEC) with strong magnetic dipolar interactions.

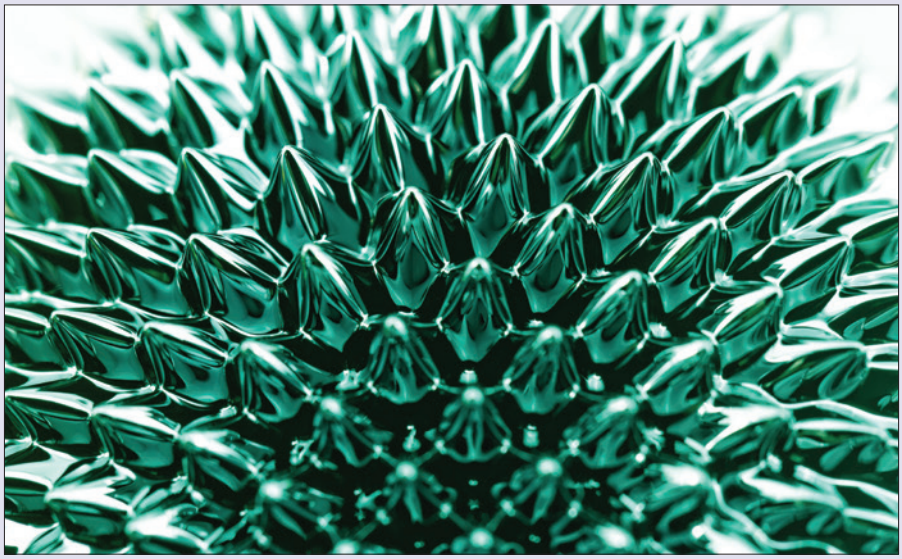

© ZOONAR GMBH / ALAMY STOCK PHOTO

The authors cooled down a gas of ^{164}Dy atoms and created a BEC of about 15,000 atoms at a temperature of 70 nK. The atoms were held in a pancake-shaped trap and subjected to an external magnetic field of approximately 0.7 mT, which aligned their magnetic moments perpendicularly to the 'pancake' containing the atomic ensemble.

The quantum Rosensweig instability resulted from the interplay between the trapping, the dipolar interactions and the contact interactions in the BEC. The latter can be tuned through Feshbach resonances, which occur when the kinetic energy of a scattering pair of atoms coincides with a bound-state energy of the atomic interaction potential. In turn, Feshbach resonances can be adjusted by varying the external magnetic field.

By using a Feshbach resonance to control interparticle interactions, Kadau *et al.* succeeded in triggering the Rosensweig instability in their dipolar dysprosium BEC. Through *in situ* imaging of the atomic density, they recorded the formation of ordered, triangular arrangements of up to ten droplets. An analysis of various realizations of such ordered structures revealed a linear increase in the number of droplets with the number of atoms, with an average of 1,750 atoms per droplet — showing that the 'droplet crystal' grew when more atoms were added.

Fourier analysis of a 2D atomic-density image provided a measure (a single number called the spectral weight) for the periodicity, or crystallinity, present in the pattern. Repeating the analysis for each image in a time sequence allowed the formation and decay times of a droplet crystal to be deduced. Kadau and colleagues found that the droplet patterns were fully developed after 7 ms, and then decayed exponentially with a mean lifetime of 300 ms. They also monitored the spectral weight when ramping the magnetic field down, and up again, and noticed differing values — hysteretic behaviour, indicative of a crystallization process.

The BEC is not only a quantum ferrofluid, but also a superfluid — at least, in the unordered phase. Whether the individual droplets display superfluidity — and hence whether the ordered system represents a supersolid state — remains an open question.

BART VERBERCK

The long and winding road

Yves Pomeau

For a problem as complex as turbulence, combining universal concepts from statistical physics with ideas from fluid mechanics has proven indispensable. Three decades since this link was formed, it is still providing food for new thought.

The pairing of stability theory with fluid mechanics dates as far back as Archimedes of Syracuse, who explained the stability of floating bodies via a geometrical method[1]. The next step came almost two millennia later, when William Thomson, later Lord Kelvin, and Hermann von Helmholtz determined that wind blowing on the sea surface makes water waves grow due to a weak instability. Shortly after, in 1883, Osborne Reynolds began systematic experimental studies of the transition to turbulence in parallel flows[2]. And now, writing in *Nature Physics*, three groups have provided the latest steps along the road to understanding how a flow transits from laminar to turbulent[3–5]. This Commentary fills the gaps on how far we have come in the past century — and where we go from here.

The early experiments inspired the introduction of what we now know as the Reynolds number, a dimensionless measure of the flow speed in a given geometry: low-Reynolds-number flows are stable and become turbulent beyond a critical value that depends on geometry. But as Reynolds seemed to understand even then, linear stability theory fails to account for all of the mysteries of fluid mechanics — the transition to turbulence in these parallel flows cannot be explained by a loss of stability with respect to fluctuations of small amplitude. For example, planar Couette flow is linearly stable at all Reynolds numbers, and is nevertheless experimentally turbulent when this number exceeds around 400–500.

Another of Reynolds's observations remained unexplained for a long time — a phenomenon he called turbulent flashes, describing the fact that parallel flows initially become turbulent in localized domains separated by laminar domains. In the 1970s, experiments showed that the turbulent patches tend to grow or decrease in size proportional to time[6,7]. This set of observations was left unexplained because it was difficult to connect it to the fundamental equations of fluid mechanics.

An original way of approaching problems in fluid mechanics was pioneered by Lev Landau in 1944[8]. His short article on the transition to turbulence followed an idea of Henri Poincaré[9], a kind of theory describing how the solutions of equations behave without solving them explicitly. This is reminiscent, however remotely, of Archimedes and his geometrical methods. The theory was initially restricted to perturbations depending on time only, but subsequent extensions included the spatial dependence of the amplitude[10–12]. In standard formulations of fluid mechanics, the fundamental object is the space- and time-dependent velocity field, which obeys the rather complex Navier–Stokes equations. Instead, the basic object in amplitude theories is a complex amplitude, describing time- and space-dependent fluctuations, in the form of nonlinear waves that may become unstable.

According to Landau, the instability can be of two different kinds: it may be supercritical, with an amplitude remaining small near the bifurcation; or it may be subcritical, with a finite amplitude at the onset of existence. This depends on the sign of a coefficient in the amplitude equation, called Landau's coefficient. In the case of instabilities of parallel flows, the instability is subcritical, which means that the amplitude of the physically observed fluctuations is never small. In the Ehrenfest classification of thermodynamic transitions, the transition to such a finite amplitude would be called first order, although the supercritical bifurcation is the equivalent of a second-order transition. In his PhD thesis, Poincaré had also classified transitions of dynamical systems, finding the equivalent of the subcritical bifurcation, which he dubbed the saddle-node bifurcation.

The physical consequences of the subcritical nature of the transition in parallel flows were not explored for some time. In the 1980s, it was shown that, depending on the Reynolds number, a localized solution surrounded by the unperturbed state grows or decays at constant speed by the motion of its boundary[13]. This growth of linearly stable amplitude fluctuations occurs by contamination for subcritical instabilities, in contrast to the supercritical case, where fluctuations grow everywhere that they are linearly unstable. This explains Reynolds's observation of 'turbulent' domains growing or decaying in an otherwise linearly stable flow. It was verified carefully in experiments by the group of Pierre Bergé and Monique Dubois[14,15], which showed that a precise onset of propagation of turbulence

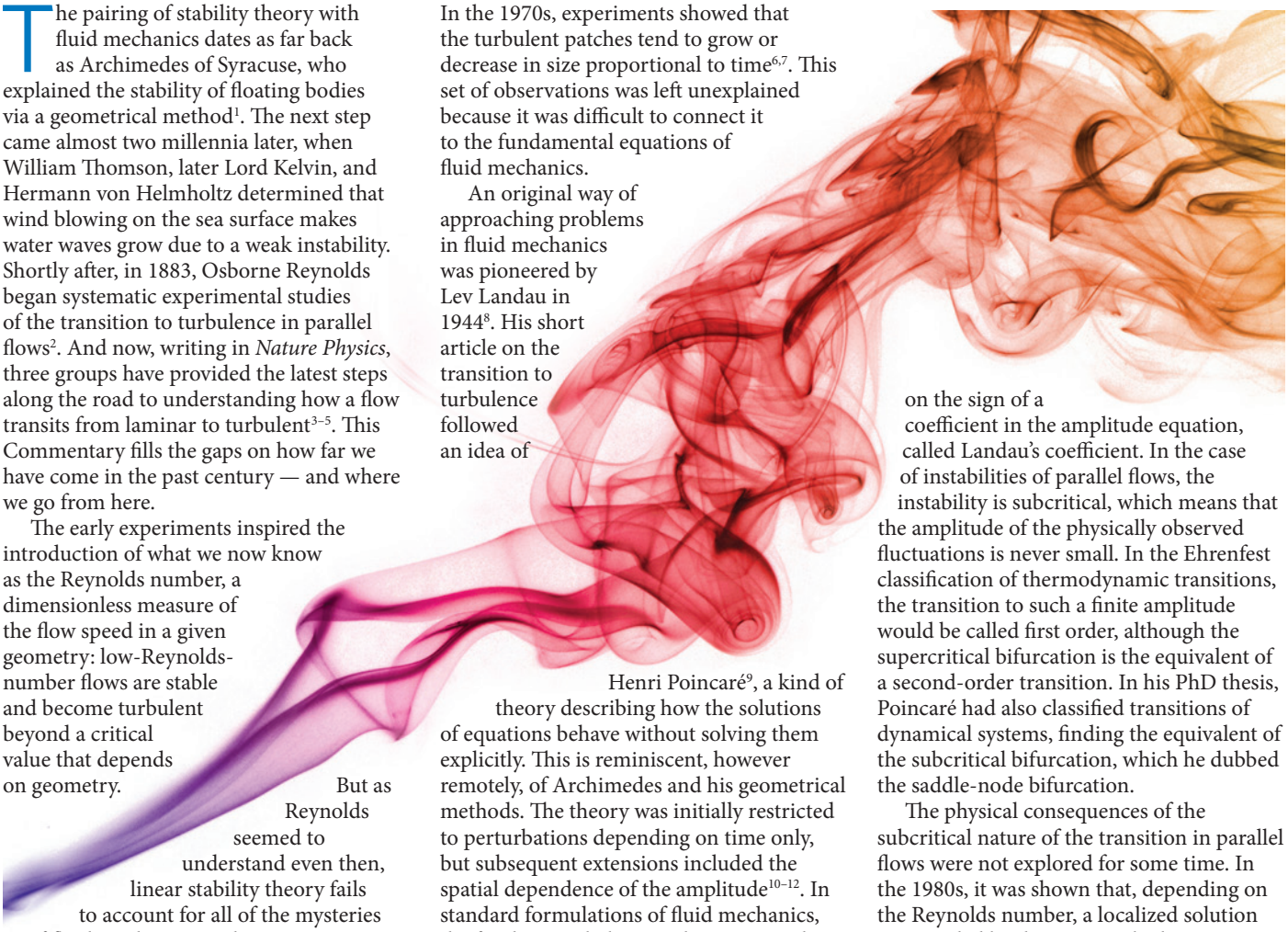

can be defined for a Couette flow and that the scenario of directed percolation was the correct one in this case.

The onset of transition to turbulence was discussed in Landau's spirit without a detailed proof, but with an explanation of the physics[13]. The problem is that amplitude theory in its original form is a mean-field theory, assuming that the inside of turbulent spots can be described as an average state. But the turbulent fluctuations inside the spots — if turbulence is there — cannot be ignored, because they can bring the flow locally and randomly back to the laminar state.

The opposite process is the expansion of the turbulent state by contamination. At the onset of the transition, the two processes balance each other out on average. At close proximity in the parameter space, contamination may win, meaning that the turbulent state wins. It loses in the opposite case, usually for lesser values of the parameter (typically the Reynolds number). Such a process is known in statistical physics as directed percolation, because the direction of time plays a special role. Time obviously plays a role distinct from that of space in this physics, because the effect of going forward or backward in time leads to a completely different result, whence the word directed. The link between the transition to turbulence and directed percolation was introduced in ref. 13. Various models showing such a transition in connection with parallel flows have followed[16,17].

In this issue of *Nature Physics,* Hong-Yan Shih *et al.*[3] have introduced a model inspired by ecology, in which various flow structures interact like species. This model, like those that came before it, is consistent with the concept that the transition is as universal as critical phenomena are in thermodynamics. And recent experimental studies, also reported in this issue, have produced spectacular space–time images of the growth of turbulent spots[4,5], which look very much like the output of the theoretical models of directed percolation. Analysis of the experiments also confirms that the exponents derived from the theory of directed percolation are the same, within the experimental error.

This may seem like the end of the story — but not quite. First, we note that a subcritical bifurcation may lead to a non-turbulent state inside the spots, which forbids us from interpreting the transition in terms of directed percolation. So the question is: does this transition belong to the universality class of directed percolation? My feeling is no. This relies on a property that is difficult to prove: namely that the bifurcation taking place at the transition either moves the system towards a turbulent or non-turbulent state. Landau-inspired theories are based on the assumption that the bifurcated state is a traveling wave of finite amplitude. However, such traveling waves may have an unstable phase — a generic instability[18–21]. So the loop is essentially closed: either the bifurcated state is stable and the transition is not of the directed-percolation type, or it is unstable and the transition is of the directed-percolation type. It is my opinion that the arrowhead patterns observed in early experiments[22] are sufficiently regular to denote a bifurcation to a turbulence-free state of finite-amplitude stable waves.

Turbulence is undoubtedly one of the hardest nuts to crack in theoretical physics. And so it is perhaps unsurprising that its progress owes very little to the exact solutions of the fundamental equations. This is best interpreted as a lesson: intuition and qualitative reasoning are often (if not always) more useful to make progress than brute force attack. Although Landau — true to his style — introduced his equation without mention of Navier or Stokes, amplitude theory was derived later in a rather systematic way from the equations of fluid mechanics. But the theory was built to stand alone, allowing for meaningful discussion without the need to derive its coefficients from the basic equations. This approach inspired new results and ideas without the cumbersome technicalities of the derivation of the amplitude equations[12]. ❐

Yves Pomeau is in the Department of Mathematics at the University of Arizona, Tucson, Arizona 85721, USA.
e-mail: pomeau@math.arizona.edu

References

1. Coullet, P. *C. R. Mecanique* **340,** 777–788 (2012).
2. Reynolds, O. *Phil. Trans. R. Soc.* **174,** 935–982 (1883).
3. Shih, H.-Y., Hsieh, T.-L. & Goldenfeld, N. *Nature Phys.* **12,** 245–248 (2016).
4. Lemoult, G. *et al. Nature Phys.* **12,** 254–258 (2016).
5. Sano, M. & Tamai, K. *Nature Phys.* **12**, 249–253 (2016).
6. Wygnanski, I. J. & Champagne, F. H. *J. Fluid Mech.* **59,** 281–335 (1973).
7. Wygnanski, I. J., Sokolov, M. & Friedman, D. *J. Fluid Mech.* **69,** 283–304 (1975).
8. Landau, L. *Doklady Akad. Nauk SSSR* **44,** 339–342 (1944).
9. Poincaré, J. H. PhD thesis, Univ. Paris (1879).
10. Segel, L. A. *J. Fluid Mech.* **38,** 203–224 (1969).
11. Newell, A. C. & Whitehead, J. A. *J. Fluid Mech.* **38,** 279–303 (1969).
12. Stuart, J. T. *Ann. Rev. Fluid Mech.* **3,** 347–370 (1971).
13. Pomeau, Y. *Physica D* **23,** 3–11 (1986).
14. Bottin, S., Daviaud, F., Manneville, P. & Dauchot, O. *EPL* **43,** 171–176 (1998).
15. Bergé, P., Pomeau, Y. & Vidal, C. in *L'Espace Chaotique* Ch. 4, 61–96 (Hermann, 1998).
16. Chaté, H. & Manneville, P. *Phys. Rev. Lett.* **58,** 112–115 (1987).
17. Barkley, D. *Phys. Rev. E* **84,** 016309 (2011).
18. Benjamin, T. B. & Feir, J. E. *J. Fluid Mech.* **27,** 417–430 (1967).
19. Benjamin, T. B. *Proc. Roy. Soc. A* **299,** 59–75 (1967).
20. Lega, J. *Physica D* **152–153,** 269–287 (2001).
21. Pomeau, Y. & Le Berre, M. Preprint at http://arxiv.org/abs/1511.08448 (2015).
22. Emmons, H. W. *J. Aero. Sci.* **18,** 490–498 (1951).

Acknowledgements

It is a great pleasure to thank Martine Le Berre for her help. Without her input, this work could have not been done.